Original Research

miR-613 suppresses renal cell carcinoma proliferation, invasion and migration by regulating the AXL/AKT pathway

Wanli Duan[1]*, Siyuan Pan[2]*, Yuyao Zhai[3], Qian Deng[1], Wei Ren[1], Chun Du[1] and Yi Sun[1]

[1]Department of Urology, Shaanxi Provincial People's Hospital, Xi'an 710068, P.R. China; [2]Xi'an Medical University, Xi'an 710068, P.R. China; [3]Department of Pharmacy, Xi'an People's Hospital, Xi'an 710004, P.R. China
*These authors contributed equally to this paper.
Corresponding author: Yi Sun. Email: sunyi3209@163.com

Impact statement

Renal cell carcinoma (RCC) is one of the most common malignant urological tumors worldwide. Thus, further exploring its treatment methods is of great significance. In this study, we explored the miR-613 mechanisms associated with anexelekto (AXL) in RCC. First, we detected miR-613 expression in RCC and its effect on patient prognosis. Next, using bioinformatics analysis, we analyzed the potential target AXL of miR-613. We discovered that AXL was inhibited by overexpression of miR-613. Finally, through rescue experiments and *in vivo* experiments, we demonstrated that miR-613 suppresses cell proliferation, invasion, and migration through the regulation of the AXL/AKT pathway in RCC. Our findings provide new evidence for the RCC regulatory mechanisms as well as the potential therapeutic targets.

Abstract

In the last few decades, microRNAs (miRNAs) are possible to effectively control and treat cancer. However, the function of miR-613 in renal cell carcinoma (RCC) is not very clear up to now. Here, the direction of this research was to investigate the influence of miR-613 for the proliferation, invasion and migration of RCC, and the underlying molecular mechanism. First, the mRNA and protein expression levels of miR-613 were determined in RCC tissues and cancer cells (786-O and ACHN). Using bioinformatics and literature review, anexelekto (AXL), as the target of miR-613 in renal cell carcinoma, was screened. Phenotype experiment and mechanism experiment illustrated the targeting relationship between miR-613 and AXL in cancer cells. Furthermore, a rescue assay with AXL overexpression was performed to make a profound study whether miR-613 disturbs RCC proliferation, invasion, and migration through direct regulation of AXL. Finally, through experiment *in vivo*, we observe the influence of miR-613 overexpression for tumor. These results were as follows. The present findings proved, in RCC, that the production of miR-613 was at a low level. Except for this point, this current research confirmed, in RCC cells, that the upregulation of miR-613 can control proliferation, metastasis, and invasion by reducing AXL levels and controlling the phosphoinositide 3-kinase (PI3K)/AKT signaling pathway.

Keywords: RCC, miR-613, AXL, AKT, proliferation, invasion, migration

***Experimental Biology and Medicine* 2023; 248: 281–292. DOI: 10.1177/15353702231151962**

Introduction

As of 2021, there were ~76,080 new cases and 13,780 new deaths in the United States annually for renal cell carcinoma (RCC).[1] In most countries and regions, the incidence of RCC is continuously increasing.[2] The clinical prognosis of metastatic RCC (mRCC) is very poor, which has a median survival time of only 13 months. Approximately 50% of patients have a survival time of <12 months, and the 5-year survival rate is 10%.[3] Treatment of advanced mRCC is a considerable clinical challenge.

In the last few decades, an ocean of research works have indicated that microRNAs are key regulatory factors related to modulation of the biological behaviors of RCC cells. Abnormally expressed microRNAs (miRNAs) participate in the initiation, development, metastasis, and drug resistance of RCC by targeting various tumor-related genes. miRNA-mediated tumor biology can provide important insights into the potential carcinogenic mechanisms of RCC, as well as novel therapeutic strategies for RCC. In fact, miRNA is a promising treatment for RCC, whether it is targeting oncogenes or tumor suppressor genes.

Studies have shown that miR-613 expression is markedly lower in gastric carcinoma, ovarian cancer, esophageal squamous cell carcinoma, osteosarcoma, liver cancer, small cell lung cancer, glioma, RCC and breast cancer, among others, relative to normal tissues, and that it can inhibit tumor proliferation, invasion and migration by targeting oncogenes such as Kirsten rat sarcoma virus (KRAS), cyclin-dependent kinase (CDK)14, CDK4, SRY-Box Transcription Factor 9, leucine zipper and EF-Hand containing transmembrane protein 1, and frizzled class receptor 7 (FZD7).[4–10] However, the functional role of miR-613 in RCC is unclear and needs to be further explored. In the study of this project, miR-613

expression was considered to be memorably downregulated in RCC, no matter in tissues and cell lines. Gain-of-function analyses demonstrated that miR-613 could be inhibited cell proliferation, invasion, and migration through targeting anexelekto (AXL). Mechanistically, this AXL/phosphoinositide 3-kinase (PI3K)/AKT signaling was supposed to be accountable to miR-613-mediated cancer suppression. This current research for these consequences provides further understanding of the aberrant molecular biological state present in RCC and improves management of this disease.

Materials and methods

Bioinformatics prediction

miR-613 was entered into the StarBase database, and its potential target was screened. Venny 2.1 was used to draw the Venn diagram of the intersection of target genes that miR-613 may regulate in the PITA, microT, miRanda, and TargetScan databases. The expression data of target genes shared by miR-613 in TCGA database were extracted. The differentially expressed genes (DEGs) in RCC and normal tissue samples screened using edgeR and DEGseq packages in R language software, and a heat map and volcano maps were drawn. Using the survival package in R, DEGs that were highly expressed in RCC and associated with poor overall survival (OS) were screened out. To detect gene expression in RCC, original gene datasets (GSE40435 and GSE53757) were downloaded from the Gene Expression Omnibus database (National Center for Biotechnology Information) and were used to analyze AXL expression. Meanwhile, the correlation between miR-613 or AXL expression and RCC survival was analyzed using the Kaplan–Meier plotter.

Study subjects

Tumor and adjacent normal tissues were obtained from 23 patients who were pathologically diagnosed with RCC by an experienced pathologist at Shaanxi Provincial People's hospital from May 2018 to May 2020. The patients registered included 17 men and 6 women aged 45–72 years. The adjacent normal tissues (5 cm from the carcinomas) were removed and used as controls. No patients had received anticancer therapies.

Materials

786-O and ACHN human RCC lines, and an HK2 normal renal tubular epithelial cell line were purchased from the Nation Collection of Authenticated Cell Cultures (Shanghai, China). Dulbecco's Modified Eagle Medium/Nutrient Mixture F-12 (DMEM/F12) medium, fetal bovine serum (FBS), penicillin, and streptomycin were purchased from Biological Industries (Israel). The lentiviral vector PLent-CMV-GFP was purchased from Jiangsu Zhenjiang Applied Biological Materials Inc. (China). Small interfering RNAs (siRNAs) against AXL were obtained from Guangzhou RiboBio Co., Ltd. (China). pcDNA3.1 plasmid containing AXL coding cDNA fragments were purchased from LMAI-Bio (Shanghai, China). SPF BALB/C4 male nude mice were purchased from Experimental Animal Center, Health Science Center, Xi'an Jiaotong University (Shaanxi, China). TRIzol® reagent was purchased from Invitrogen (Thermo Fisher Scientific, Waltham, Massachusetts, United States). A FastKing RT Kit (with gDNase) was purchased from TIANGEN Company (cat. no. KR116; Beijing, China). A ChamQ Universal SYBR qPCR Master Mix (cat. no. Q711-02) was purchased from Vazyme Biotech (China). Cell counting kit-8 (CCK-8. cat. no. C0039) apoptosis and proliferation kits were purchased from Shanghai Beyotime Biotechnology Co., Ltd. (China). A transwell chamber was purchased from Corning Inc. (cat. no. 3495; Somerville, MA, USA) and Matrigel® (cat. no. 354230) was purchased from Becton, Dickinson and Company (Franklin Lakes, NJ, USA). Radioimmunoprecipitation assay buffer (RIPA) buffer (high) (cat. no. R0010) and a bicinchoninic acid assay (BCA) kit (cat. no. PC0020) were purchased from Beijing Solarbio Science & Technology (China). AXL (WB:1:1000, IHC:1:200, cat. no. ab130218), AKT(WB:1:1000, cat. no. ab8805), Phospho-AKT (WB:1:1000, cat. no. ab38449), and β-actin (WB:1:5000, cat. no. ab8227) antibodies, as well as reverse transcription and polymerase chain reaction (PCR) kits, were purchased from Abcam (Cambridge, UK). Horseradish peroxidase (HRP)–labeled goat antimouse IgG (1:5000 cat. no. BA1050) and goat antirabbit IgG (1:5000 cat. no. BA1054) antibodies were purchased from Wuhan Boster Biological Technology (China).

Cell grouping and transfection

The HK-2 cells, 786-O and ACHN cells were cultured in DMEM/F12 medium at 37°C and 5% CO_2. A lentiviral vector containing miR-613-specific overexpression fragment (pLen-CMV-GFP) and negative control empty virus vector were transfected into two RCC cells, comprising the Lenti-miR-613 and Lenti-miR-NC groups, respectively. For AXL overexpression and knockdown, AXL pcDNA or small-interfering RNAs (siRNAs) were transfected into cells using Lipofectamine 3000.

Reverse transcription-quantitative polymerase chain reaction for miR-613, AXL quantification

Total RNA was extracted from tumor tissues and cells using TRIzol reagent (Thermo Fisher Scientific) and reverse-transcribed into cDNA (TIANGEN, Beijing, China). ChamQ Universal SYBR qPCR Master Mix (Vazyme Biotech) were prepared in accordance with the manufacturer's instructions for a reverse transcription-polymerase chain reaction (RT-PCR) reaction. The relative expression was calculated using the $2^{-\Delta\Delta CT}$ method. The primers used are shown as follows: miR-613 (forward 5′-CTTCGTCGGCTCTTCCATACATACT-3′; reverse 5′-TTCACTTAGATACAGCTACGT-3′); U6 (forward 5′-CTCGCTTCGGCAGCACATAT-3′; reverse 5′-TTGCGTG TCATCCTTGCG-3′); AXL (forward 5′-AGCACACGCGTA AACAACAC; reverse GTTATGGGCTTCGCAGGAGA-3′); β-actin (forward 5′-CATGTACGTTGCTAT CCAGGC-3′; and reverse 5′-CTCCTTAATGTCACGCACGAT-3′).

Western blotting

Equal amounts of protein were separated by sodium dodecyl-sulfate polyacrylamide gel electrophoresis (SDS-PAGE) and transferred onto a polyvinylidene difluoride (PVDF)

membrane, confined with 5% bovine serum albumin, and incubated with AXL, p-AKT, AKT (Abcam), or β-actin primary antibodies at 4°C overnight. The second day, HRP-labeled secondary antibodies were added for incubation at room temperature for 1 h. Finally, luminescent liquid was added, followed by exposure and photographing using a gel imager. The gray scale value was recorded, and the relative expression level was calculated.

Dual-luciferase reporter assay

The predicted binding site in AXL was subcloned into the pmirGLO vector (Promega, Madison, WI, United States). Using Lipofectamine 3000 (Invitrogen), pmirGLO vectors containing AXL wild-type (WT) or mutant-type (MT) 3′-UTR cells were co-transfected into 786-O cells with miR-613 mimics or miR-NCs. Dual-luciferase activity was measured 48 h after transfection using the dual-luciferase reporter system method.

Cell proliferation analysis

A CCK-8 (TransGen Biotech Co., Ltd., Beijing, China) was adopted to examine cell proliferation. Cells were cultured in 96-well plates ($n = 6$ per group). Cells were cultured for 24 h, and 10 μL CCK-8 solution was then added to each well and mixed with 40 μL DMEM/F12 medium to set six blank control wells. Both were incubated in a cell incubator for 2 h. At 450 nm, the absorbance of each secondary well was measured.

Transwell assay

The basement membrane apical compartment was coated with Matrigel (1:8 dilution) and dried at room temperature. Following conventional digestion, cells were suspended in DMEM/F12 medium, and cell density was adjusted to 1×10^5 cells/mL. Next, 150 μL cell suspension was added to the top chamber of the transwell chamber covered with Matrigel, and 500 μL of DMEM/F12 medium rich in 20% FBS would be poured into the basolateral room. After 24 h of regular culture, cells were first fixed with 4% paraformaldehyde, and then stained with 0.5% crystal violet solution. Cells that transmembrane were counted. Also, in the experiment, three subholes were provided for each experimental group, respectively.

Colony formation assay

Aliquots of 1×10^3 cells would be cultured into six-well plate. Each clone was stained with crystal violet dye after seven days of culture. The experiment was carried out three times. Cells would be fixed with methanol and stained with 0.5% crystal violet. In the end, taking picture by camera, the colonies were counted.

Immunohistochemistry

After obtaining the tumor body of nude mice, part of the tissue was fixed with 40% (volume fraction) formalin. The appropriate size of tissue (about 2 mm thick) was cut for embedding. The ethanol and xylene solution were dehydrated. The xylene solution dewaxed the paraffin embedded sample, and the gradient ethanol and distilled water were hydrated layer by layer. After being treated with citrate buffer solution (pH 6.0), the antigen was repaired in microwave oven (high temperature for 2 min, medium temperature for 8 min). The normal goat serum was blocked for 20 min, incubated with the primary antibody at 4°C overnight. Next, the counterpart of secondary antibody and 3,3′-diaminobenzidin (DAB) were color treated. Hematoxylin was re-stained, dehydrated, and sealed. The specimens were confirmed by two pathologists. Under the light microscope, the cells with brown yellow granules in the cytoplasm or nucleus are positive cells. Then, using Image-Pro Plus 6.0 software, image optical density was conducted quantitative analysis.

Xenograft studies

Nude mice ($n = 12$) were separated into two groups ($n = 6$ per group). 786-O cells transfected with Lenti-miR-NC and Lenti-miR-613 were injected into the underarm of the mice in each group at ~1×10^6 cells/200 μL/per mouse. At the end of the third week, 12 nude mice were anesthetized by inhalation of 3% isoflurane and sacrificed by cervical dislocation. Death was verified by the absence of a heartbeat and respiration. All mice were euthanized. Finally, the transplanted tumor was dissected and weighed.

Statistical analysis

The Wilcox test was used to screen the DEGs in TCGA database, and FoldChange (FC) was processed by log2. Univariate Cox regression analysis was performed to screen genes with different prognosis. Other data were processed using SPSS 25.0 statistical software (IBM, Armonk, NY, USA) and presented as the mean value ± standard deviation. A *t*-test was used to evaluate the two groups, and one-way analysis of variance was used for multiple-group comparisons. Pairwise comparisons between multiple groups were performed using a Tukey's post hoc test, and data at different time points were compared by repeated measures analysis of variance (ANOVA). $P < 0.05$ was considered as a statistically significant difference.

Results

miR-613 expression in renal clear cell carcinoma and its effect on patient prognosis

Using reverse transcription-quantitative polymerase chain reaction (RT-qPCR), the expression of endogenous miR-613 for human RCC tissues and contiguous non-cancerous tissues was compared. The results (Figure 1(A); $P < 0.01$) showed that the expression level about miR-613 inside the human RCC tissue was noticeably lower than which for surrounding and adjacent non-tumor tissues. miR-613 expression would be then examined in 786-O, ACHN, and HK2. miR-613 was expressed at lower level in two RCC cells (Figure 1(B); $P < 0.05$). miR-613 overexpression was found to be positively correlated with OS for almost all of RCC patients in the Kaplan–Meier plotter database (Figure 1(C); $P < 0.001$).

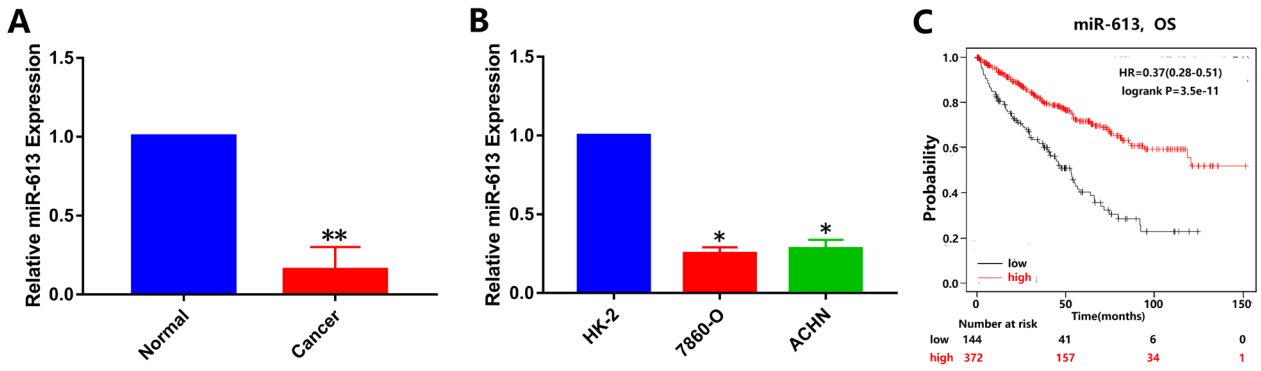

Figure 1. miR-613 expression in renal clear cell carcinoma and its effect on patient prognosis. (A) RT-qPCR detected lower miR-613 expression level in RCC tissues than in the adjacent non-neoplastic tissues. $^{**}P < 0.01$ versus adjacent non-neoplastic tissues. (B) RT-qPCR detected the miR-613 expression in 786-O and ACHN cells. HK-2 cells were used as the control cell line. $^{**}P < 0.05$ versus HK-2. (C) OS survival curves of RCC ($n = 516$).
OS: overall survival.

Effect of miR-613 on proliferation, invasion, and migration in RCC

For the sake of clarity, the potential influence of miR-613 in RCC, miR-613 overexpression on RCC cellular processes was detected following transfection with lentivirus with miR-613 mimics into 786-O and ACHN cells, which displayed that the miR-613 was overexpression (Figure 2(A); $P < 0.001$). This assay of CCK-8 outcomes illustrated that Lenti-miR-613 mimics markedly disturbed the proliferation of RCC cell lines, in which it was compared with control and Lenti-miR-NC cells (Figure 2(B) and (C); $P < 0.001$). The colony formation assay demonstrated that miR-613 overexpression significantly inhibited RCC cell colony–forming ability (Figure 2(D) and (E); $P < 0.01$). As shown by the migration and invasion assays, a clear decline in terms of cell number was observed following transfection with Lenti-miR-613 mimics (Figure 2(F) to (I); all $P < 0.01$).

Screening of targets and pathways of miR-613 in RCC using bioinformatics

The above experiments have confirmed that miR-613 restrains the proliferation, invasion, and migration for the human RCC cell lines, but the underlying molecular mechanism remains unclear. For the reason to select genes targeted by miR-613 in RCC, 2753 target genes which might be subjected by miR-613 were downloaded from several databases, including the PITA, microT, miRanda, and TargetScan in StarBase website. The genes regulated by miR-613 in four gene data sets were compared to one another, and a Venn diagram was generated (Figure 3(A)). The Venn diagram revealed 239 intersecting genes. A total of 539 RCC tissue samples and another 72 normal tissue samples were downloaded from the TCGA database, and the clinical information of 537 patients with RCC was downloaded. Out of these 239 intersecting genes in TCGA database, 37 DEGs were screened out (the screening criteria were: $|\log2FC| > 1$ and $P < 0.05$), 20 of which were upregulated and 17 downregulated (Figure 3(B) and (C)). Using the survival package of the R software, 10 DEGs that had the potential to affect the OS time of patients were screened out from the 20 upregulated DEGs ($P < 0.05$), of which 8 were highly expressed (AC008878.3, brain-derived neurotrophic factor, engulfment and cell motility 1, ETS proto-oncogene 1, transcription factor, neuropilin 1, annexin A4, gap junction protein α 1, and endothelin 1) and associated with a better survival time, and 2 (AXL and SH3 domain-binding glutamate rich protein-like 3 [SH3BGRL3]) were associated with a worse OS (Figure 3(E); $P < 0.05$). The gene functions of AXL and SH3BGRL3 were explored in the GeneCard database (https://www.genecards.org/), and it was found that SH3BGRL3 could act as a modulator of glutaredoxin biological activity. AXL could regulate numerous physiological processes, for instance, cell survival, cell proliferation, migration, and differentiation. Subsequently activation by ligand, AXL combines and leads to the tyrosine phosphorylation of PI3-kinase subunits PIK3R1, PIK3R2, and PIK3R3. Previous studies have found that AXL receptor tyrosine kinase is a potential therapeutic target for RCC.[11,12] We hypothesized that miR-613 suppresses RCC proliferation, invasion, and migration through targeting AXL to the PI3K/AKT signaling pathway.

miR-613 directly targets AXL mRNA and suppresses the activity of the PI3K/AKT signaling pathway

The association between AXL and miR-613 in 786-O cell lines was discussed. The putative sites were bound between miR-613 and AXL (Figure 4(A)). In 23 cases of RCC, correlation analysis showed that there was a significant negative correlation between AXL and miR-613 (Figure 4(B)). To verify the hypothesis, 786-O-Lent-miR-613 and 786-O-Lent-miR-NC cells were transfected with the constructs of wild-type promoter (pGL3-AXL-WT) or the promoter with mutations in the binding site (pGL3-AXL-MT) for 48 h. miR-613 overexpression was found to decrease the expression of pGL3-AXL-WT. Meanwhile, when the putative miR-613 binding site of pGL3-AXL-WT was destroyed, its role was restrained (Figure 4(C)). Furthermore, no matter the cellular mRNA (Figure 4(D)) or protein levels (Figure 4(E) to (H)), miR-613 overexpression markedly decreased the expression of AXL. This finding indicated that AXL should be considered the target of miR-613. AXL could lead to the tyrosine phosphorylation of PI3-kinase subunits PIK3R1, PIK3R2, and PIK3R3. PI3K/AKT signaling pathway activation is very essential to be correlated with the aggressive development for RCC and poor

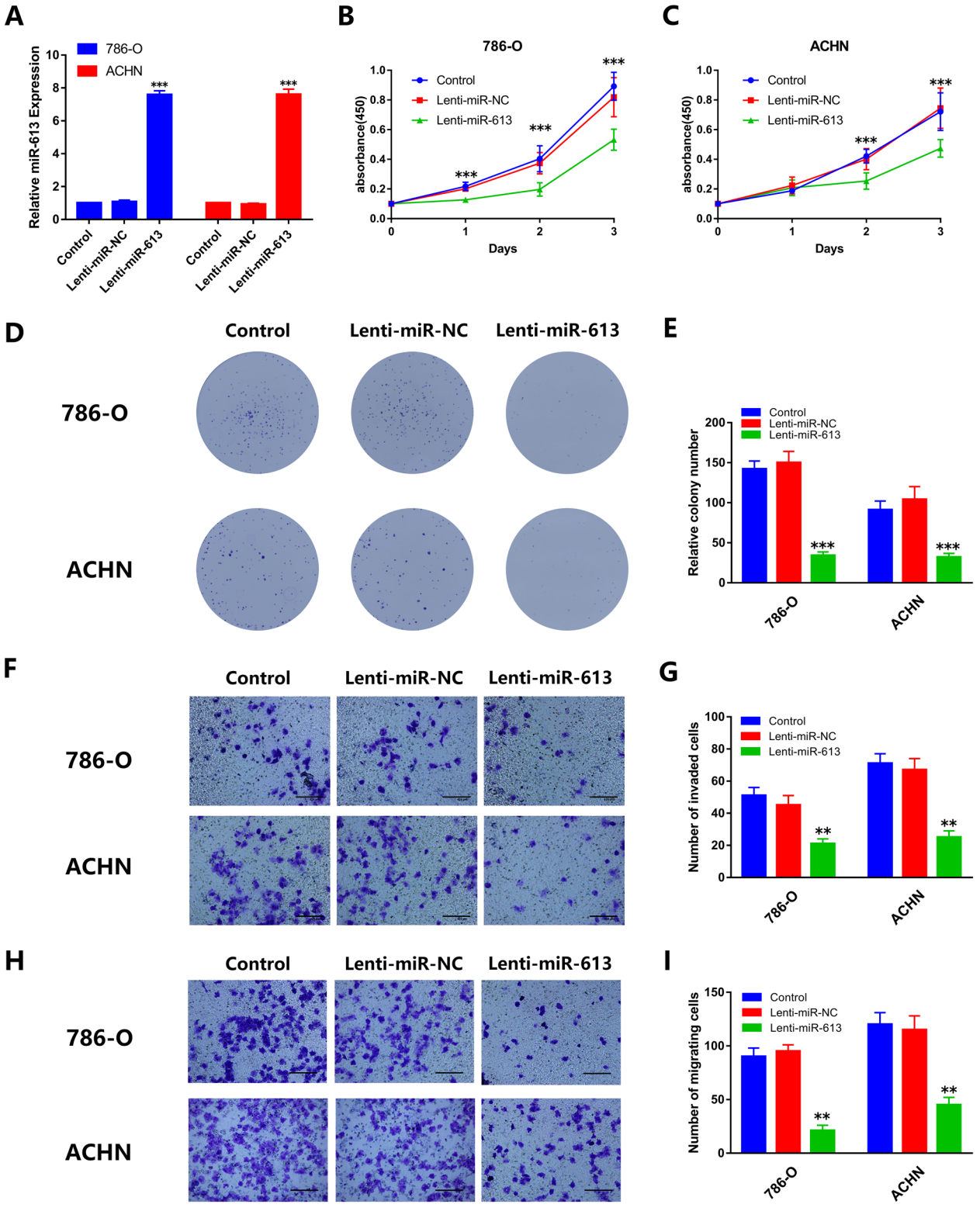

Figure 2. miR-613 negatively regulates RCC cells. (A) RT-qPCR checked miR-613 expression in 786-O and ACHN cells following transfection with lentivirus with miR-613 mimics or negative control empty virus vector. ***$P < 0.001$ versus control or Lenti-miR-NC. (B and C) A CCK-8 assay was performed to examine cell proliferation in 786-O and ACHN cells treated with Lenti-miR-613 mimics or Lenti-miR-NC for 24, 48, and 72 h. ***$P < 0.001$ versus control or Lenti-miR-NC. (D and E) After 14 days of incubation, the colony formation assay was used to detect cell proliferation in 786-O and ACHN cells treated with Lenti-miR-613 mimics or Lenti-miR-NC. ***$P < 0.01$ versus Lenti-miR-NC or control. (F to I) A transwell invasion assay was performed to evaluate the invasion and migration abilities of 786-O and ACHN cells treated with miR-613 mimics or miR-NC. *$P < 0.01$ versus control or Lenti-miR-NC. Ruler scale = 50 μm.

survival.[13] A previous study examined how PI3K inhibitors affected the proliferation, invasion, and migration of RCC. LY294002 is a widely used PI3K inhibitor that could be used to bind to the PI3K active site which could be competed with adenosine triphosphate (ATP).[14] Using CCK-8 assays, it was confirmed that inhibiting PI3K with LY294002 significantly

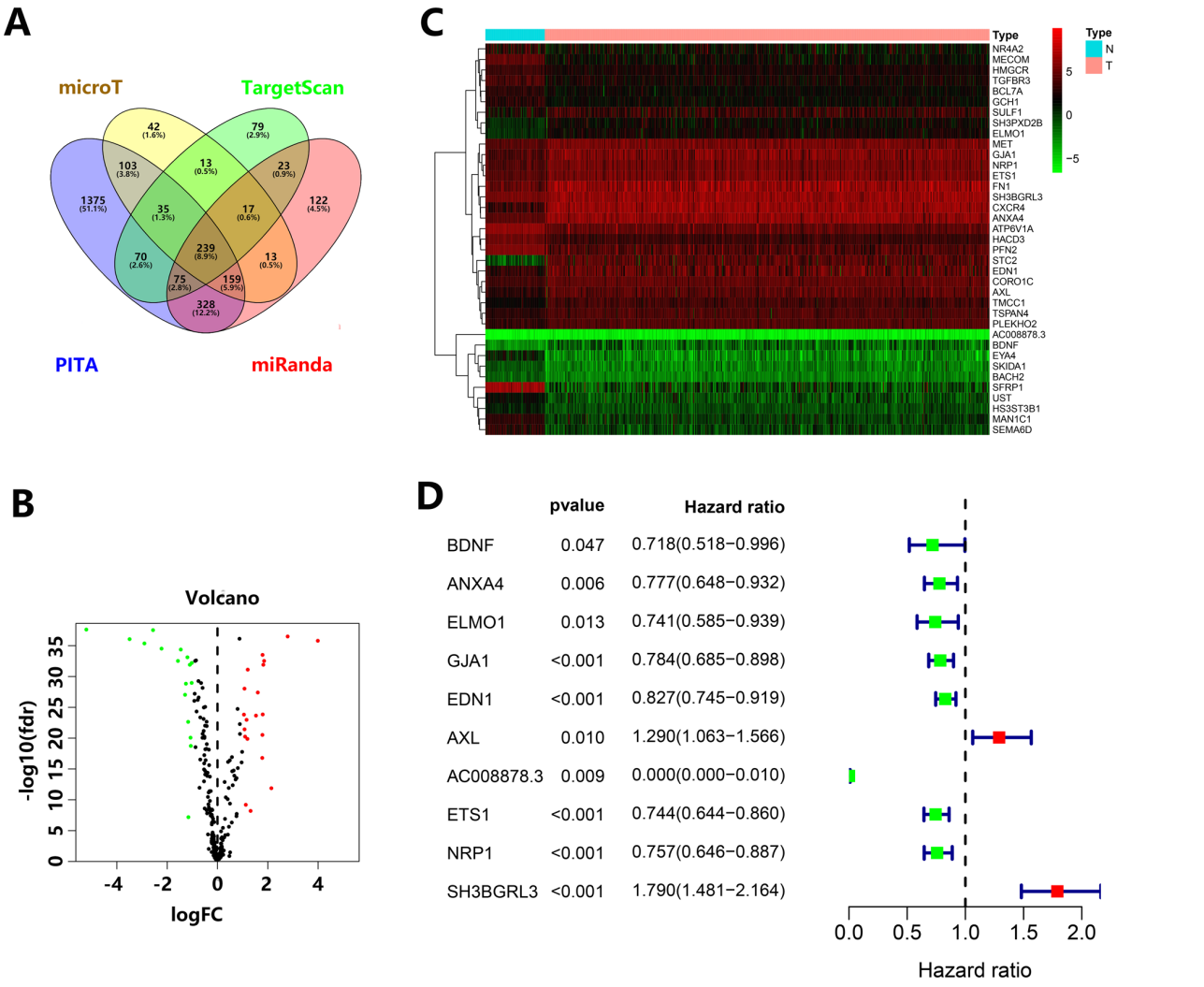

Figure 3. Screening of targets and pathways of miR-613 in RCC using bioinformatics. (A) The potential target genes of miR-613 were screened in the PITA, microT, miRanda, and TargetScan databases, and 239 intersecting genes were found. (B) Analysis of a volcano map of DEGs. The red dots represent 20 upregulated DEGs, the green dots represent 17 downregulated DEGs, and the black dots represent genes that are not differentially expressed in RCC tissues. (C) Heat map analysis of the differential expression of the 239 intersecting genes in kidney cancer and normal tissues. (D) Univariate Cox regression analysis of the risk characteristics of 20 upregulated DEGs associated with renal cancer prognosis.
DEG: differentially expressed gene.

reduced cell proliferation (Figure 4(I) and (J)). Furthermore, through using the transwell assay, LY294002 revealed that it could inhibit cell invasion and migration in RCC cell lines (Figure 4(K) to (N)). These consequences proved that the inhibition of the PI3K/AKT signaling pathway is a good way to inhibit the proliferation, invasion, and migration in RCC cell lines. For the sake of ensuring the potential mechanism, the influence of miR-613/AXL upon activation of PI3K/AKT signaling was investigated. So, the rate of p-AKT/AKT was markedly decreased (Figure 4(E) to (H)), when miR-613 was overexpressed in 786-O or ACHN cells, which indicated that miR-613 could have the potential mechanism to induce and disturb the stimulation of PI3K/AKT pathway.

AXL expression and its influence on patient prognosis in RCC

In addition to TCGA gene data set, AXL was also overexpressed in tumor tissues in the GSE40435 and GSE53757 gene data sets (Figure 5(A)). To further study the expression of AXL in RCC cells, the human RCC tissue and the adjacent normal tissue were tested the expression of AXL using RT-qPCR and western blotting. It turned out that the AXL mRNA and protein relative expressions were markedly higher ($P < 0.01$) in RCC (Figure 5(B) to (D)). For the sake of deep research, the correlation and potential mechanisms of AXL expression in RCC, the association in the Kaplan–Meier plotter databases between AXL expression and prognosis was investigated in patients with RCC. RCC overexpression was positively correlated to a poor OS and progression-free survival (PFS) in RCC patients (Figure 5(E) and (F); $P < 0.05$).

AXL downregulation inhibits RCC cell proliferation, migration, and invasion via PI3K/AKT signaling

The role of AXL was identified, and the expression of AXL was found to be inhibited by siRNA. In siRNA-transfected cells, the AXL mRNA (Figure 6(A)) and protein expressions

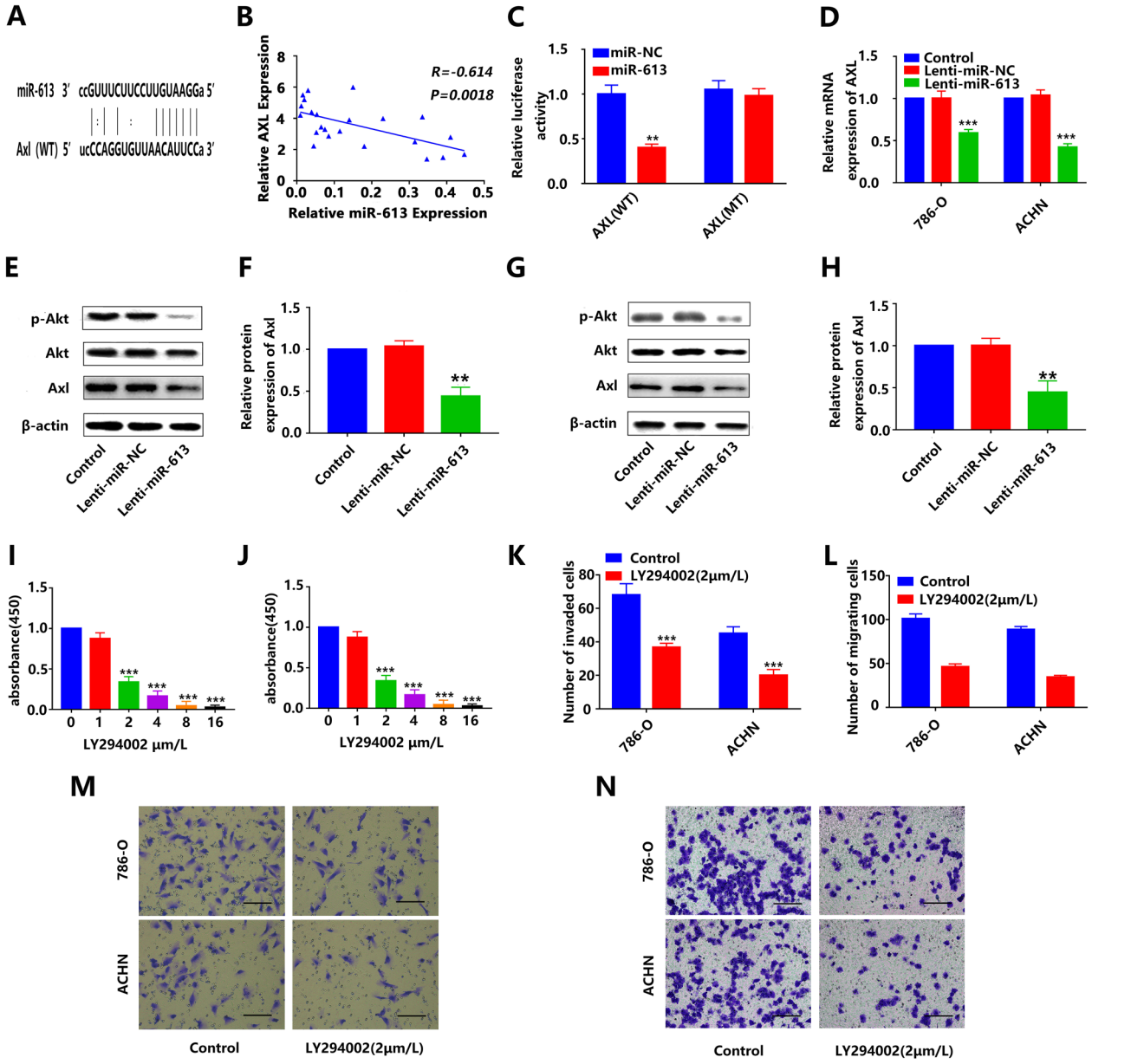

Figure 4. Directing the interaction between miR-613 and AXL. (A) Sequences of putative miR-613 binding sites in the 3'-UTR of AXL. (B) Statistical relationship between the expression of miR-613 and AXL in tumor tissues of 23 patients ($R=-0.614$, $P<0.001$). (C) To confirm the direct association between miR-613 and the 3'-UTR of AXL, a dual-luciferase activity assay was used. (D) The AXL mRNA expression level was detected in 786-O and ACHN cells following transfection with lentivirus containing miR-613 mimics or negative control empty virus vector. (E to H) Western blotting was performed to detect the protein level of AXL, AKT, and p-AKT in 786-O and ACHN cells following transfection with lentivirus containing miR-613 mimics or negative control empty virus vector. (I and J) The effect of LY294002 on 786-O and ACHN cell proliferation was assessed using a CCK-8 assay at 24 h. (K and M) The effect of LY294002 on the invasive ability of 786-O and ACHN cells was measured using a transwell invasion assay after 24 h of incubation. (L and N) The effect of LY294002 on the migration ability of 786-O and ACHN cells was assessed using a transwell migration assay after 24 h of incubation. Ruler scale = 50 μm.
$^{**}P<0.01$; $^{***}P<0.001$.

(Figure 6(B) to (D)) were markedly inhibited following AXL gene knockdown. The CCK-8 assay (Figure 6(F)) revealed that AXL knockdown instantly repressed cell growth. The transwell assay demonstrated a significant cell invasion (Figure 6(G) and (I)) and migration (Figure 6(H) and (J)) inhibition in the siRNA-transfected cells compared with control- and siRNA-NC-transfected cells. Thus, it seems that AXL knockdown increased cell proliferation, invasion, and migration. The rate of p-AKT/AKT was markedly decreased following the downregulation of AXL (Figure 6(B), (C), and (E)). These results indicated, in RCC, AXL regulates certain physiological processes by activating PI3K/AKT signaling.

The inhibitory effect of miR-613 proliferation, invasion, and migration, as weak as PI3K/AKT signaling activity in RCC cells, was reversed by AXL overexpression

A rescue assay with AXL overexpression was performed whether miR-613 inhibits various characteristics of RCC

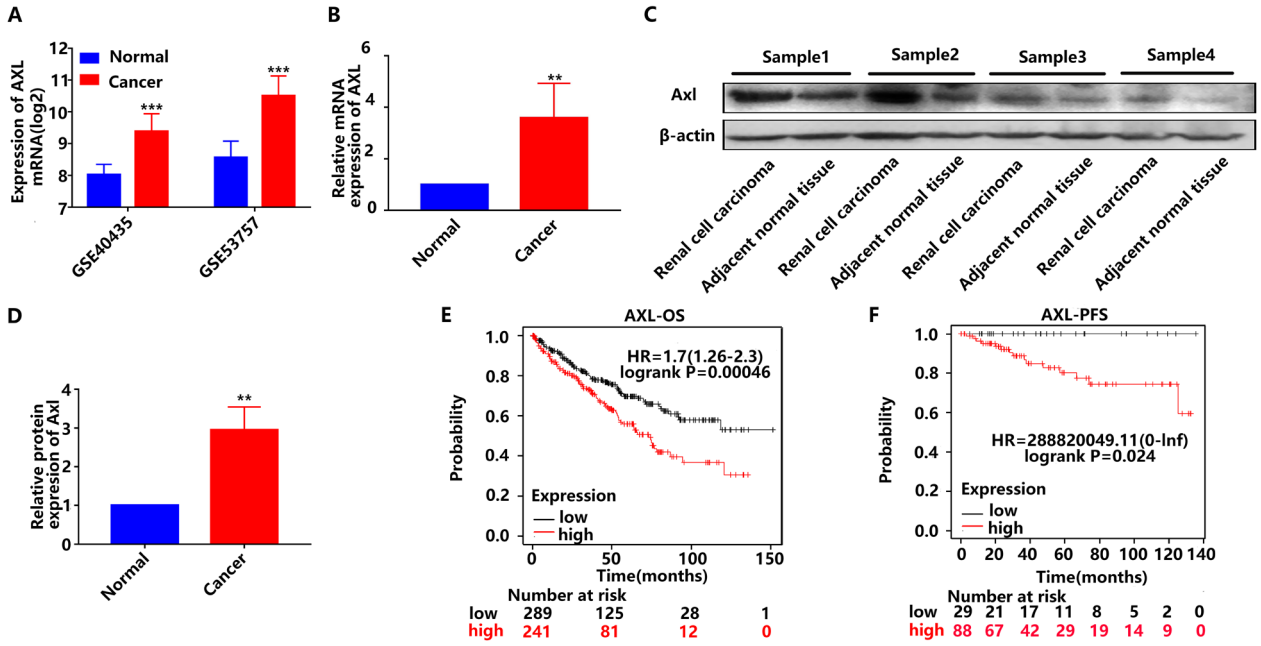

Figure 5. AXL is upregulated in RCC tissues. (A) AXL expression in the gene data sets GSE40435 and GSE53757. (B) RT-qPCR detected the AXL mRNA expression level in RCC and adjacent normal tissues in 23 patients with RCCC. (C and D) Western blotting was performed to assess the protein level of AXL in 23 patients with RCC. (E and F) Overall survival and disease-free survival curves of RCC ($n=530$, $n=117$).
*$P<0.05$; **$P<0.01$; ***$P<0.001$ versus adjacent normal tissue.

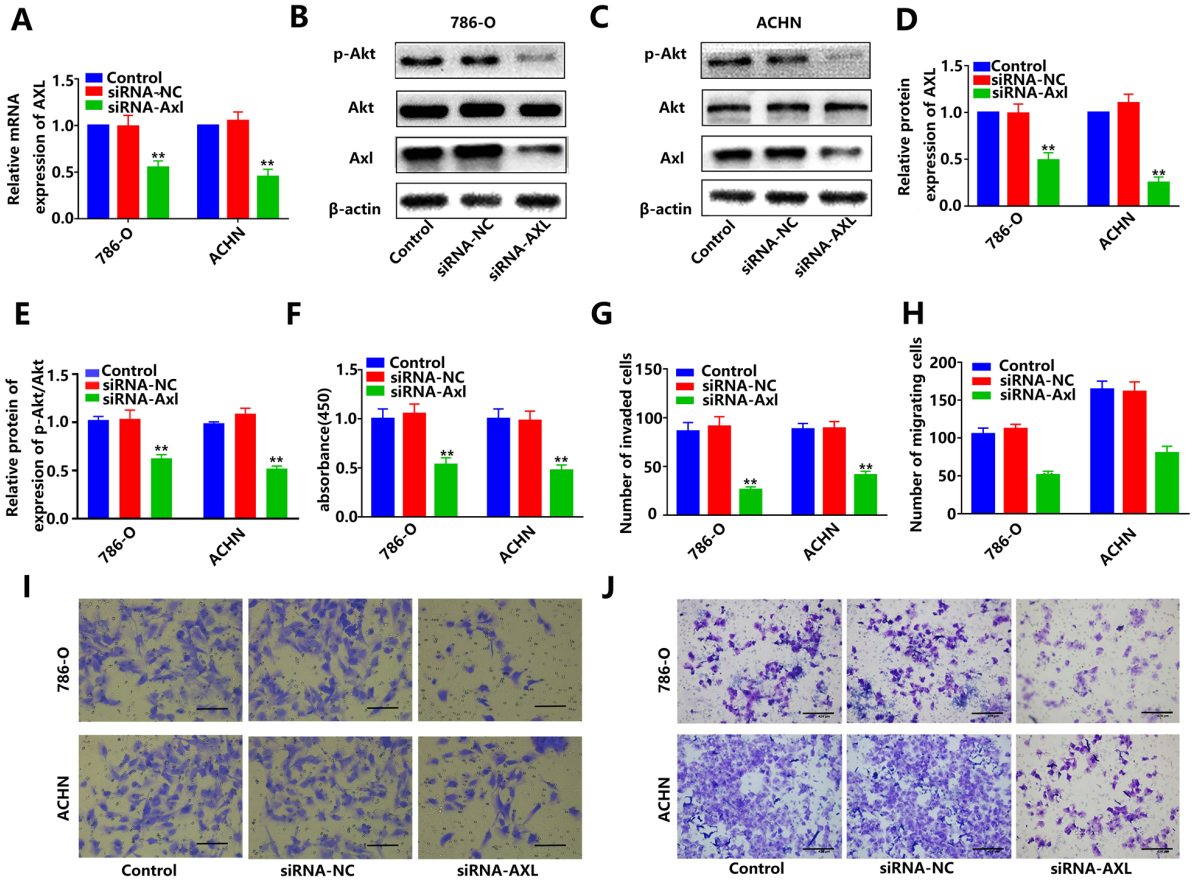

Figure 6. AXL regulates RCC cell growth, invasion, and migration. (A) RT-qPCR detected AXL mRNA expression in 786-O and ACHN cells transfected with AXL siRNA for 48 h. (B to E) Western blotting detected the protein level of AXL, AKT, and p-AKT in RCC cells transfected with AXL siRNA for 48 h. (F) The effect of AXL siRNA transfection on 786-O and ACHN cell proliferation was assessed using a CCK-8 assay at 48 h. (G and I) Using a transwell invasion assay after 24 h of incubation, the effect of AXL siRNA transfection on the invasive ability of 786-O and ACHN cells was measured. (H and I) The effect of AXL siRNA transfection on the migration ability of 786-O and ACHN cells was assessed using a transwell migration assay after 24 h of incubation. *$P<0.05$ versus NC siRNA or NC shRNA. *$P<0.01$ versus siRNA-NC or control. Ruler scale = 50 μm.

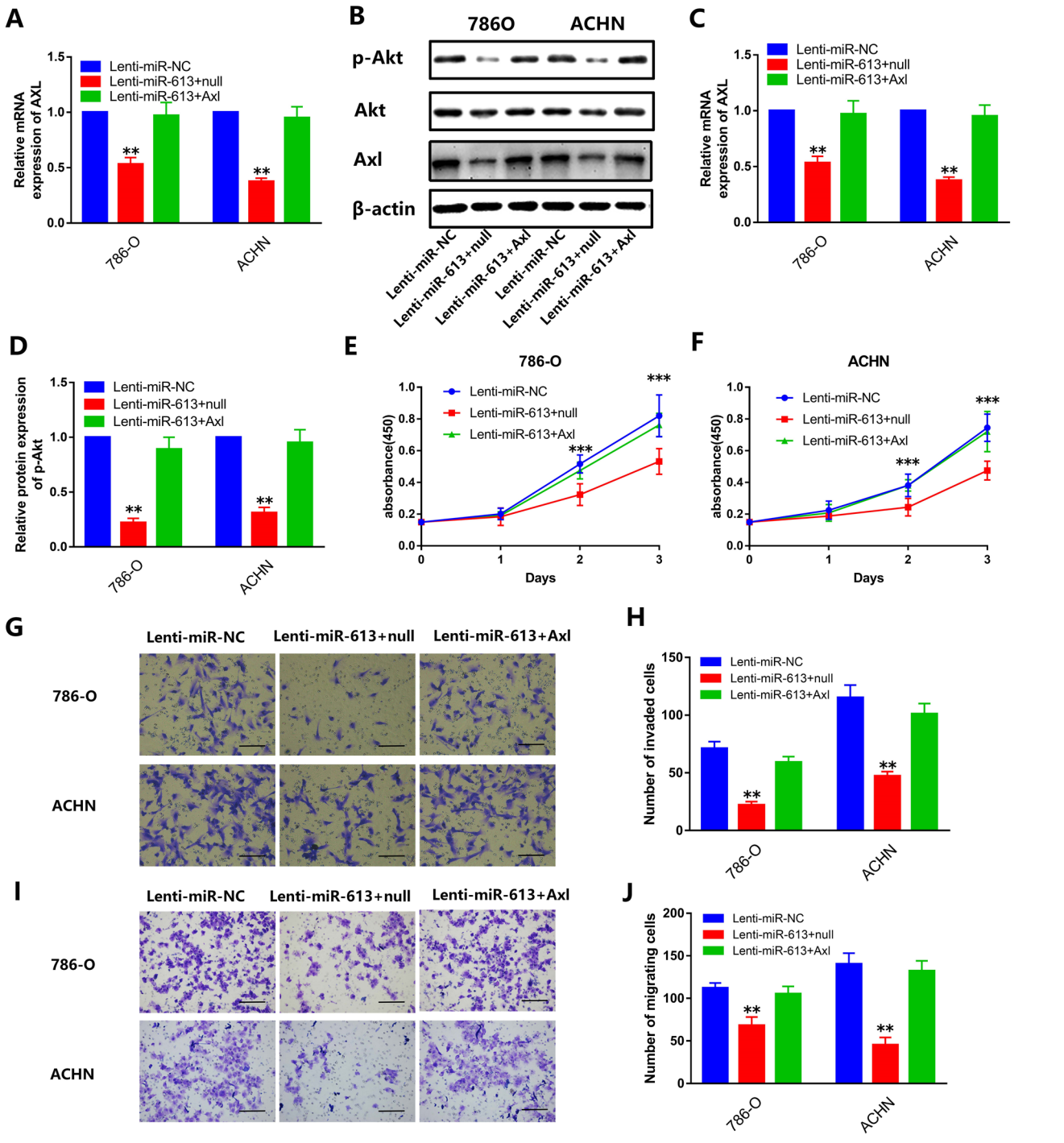

Figure 7. In RCC cells, the restoration of AXL expression reversed the antitumor effect of miR-613. Lenti-miR-613 mimics and either the pcDNA3.1/AXL expression vector or the pcDNA3.1 empty vector was co-transfected into 786-O and ACHN cells. Null vectors were empty vectors. (A) AXL mRNA expression was measured using RT-qPCR after 48 h of transfection with pcDNA3.1/AXL expression vector or pcDNA3.1 empty vector. (B and D) The protein expression of AXL, AKT, and p-AKT after 48 h of transfection with pcDNA3.1/AXL expression vector or pcDNA3.1 empty vector. (E and F) Cell proliferation was measured using a CCK-8 assay after 24, 48, and 72 h of transfection with the pcDNA3.1/AXL expression vector or the pcDNA3.1 empty vector. (G and H) After 24 h of transfection with the pcDNA3.1/AXL expression vector or the pcDNA3.1 empty vector, cell invasion was measured using the transwell invasion assay. (I and J) After 24 h of transfection with the pcDNA3.1/AXL expression or the pcDNA3.1 empty vector, cell migration was assessed using a transwell migration assay. Lent-miR-613 mimic + AXL versus Lent-miR-613 mimic + null, $^{**}P < 0.01$; $^{***}P < 0.001$. Ruler scale = 50 μm.

through direct regulation of AXL. Two RCC cells were co-transfected both the Lenti-miR-613 mimic and AXL. So detected by RT-qPCR (Figure 7(A)) and western blotting (Figure 7(B) and (C)), miR-613-induced AXL overexpression was reversed by transfection with AXL-expressing vector in 786-O and ACHN cells. As expected, AXL overexpression markedly rescued the inhibited effect on miR-613 proliferation (Figure 7(E) and (F)), invasion (Figure 7(G) and (H)), and migration (Figure 7(I) and (J)) in RCC cells. In addition, in two RCC cell lines, the decline in PI3K/AKT signaling pathway activity following AXL overexpression partially reversed during miR-613 overexpression (Figure 7(B) and (D)).

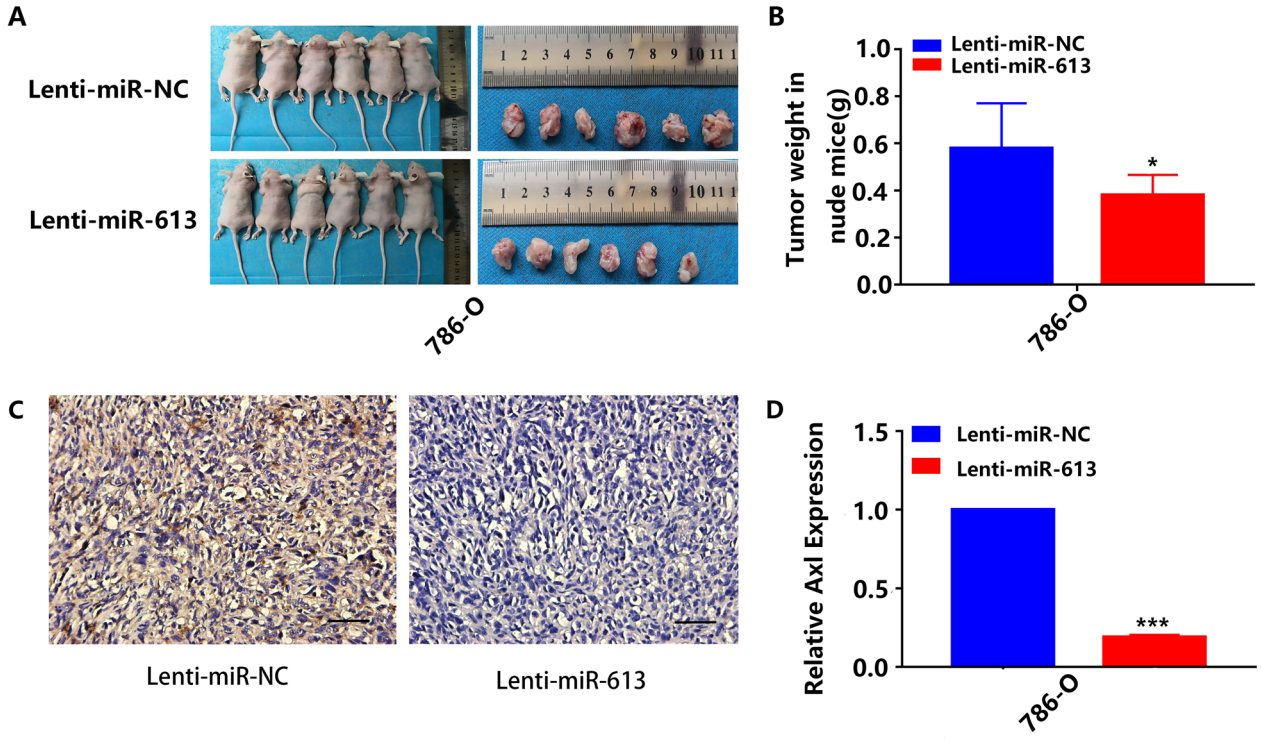

Figure 8. miR-613 overexpression attenuates tumor growth *in vivo*. (A) Effect of miR-613 overexpression on tumor volume in nude mice. (B) Effect of overexpression of miR-613 on tumor weight in nude mice. (C) Immunohistochemical test was used to detect the expression of AXL in tumor tissues of nude mice under miR-613 overexpression. (D) Effect of miR-613 overexpression on the relative expression of AXL in tumor tissues of nude mice. $^{*}P < 0.05$; $^{***}P < 0.001$. Lent-miR-613 versus Lent-miR-NC. Ruler scale = 50 μm.

miR-613 overexpression attenuates tumor growth *in vivo*

For the reason to decide whether miR-613 could regulate AXL expression and suppress RCC cell proliferation, it was examined whether this antineoplastic miRNA had a similar effect *in vivo*. A nude mouse xenograft model was used. 786-O cell lines that stably transfected with Lent-miR-613 NC and Lent-miR-613 mimic, both of them were injected into the underarm of the nude mice. Three weeks after inoculation, the largest tumor observed was ~14 mm. This finding showed that miR-613 can inhibit RCC growth (Figure 8(A) and (B)). Through immunohistochemistry experiment on tumor tissue of nude mice, it was further proved that the production of AXL was dramatically disturbed due to the overexpression of miR-613 *in vivo* (Figure 8(C) and (D)).

Discussion

AXL, also known as Ufo, Ark, JTK11 and Tyro-7, originated from the ancient Greek word "anexelekto," meaning "excessive and uncontrollable." The AXL gene is located at q13.2 of chromosome 19 and belongs to the TAM (TYRO3-AXL-MER) family of receptor tyrosine kinases. From solid to liquid tumors, AXL is involved in variously malignant tumors, such as cell growth, proliferation, survival, apoptosis, and adhesion. A previous study found that AXL is overexpression in numerous human neoplasia,[15] and is closely connected with their occurrence, development, and even drug resistance. Reducing the expression of AXL kinase or blocking its kinase activity can inhibit the growth, invasion, and metastasis for these cancer cells.[16–20] The detection that the expression of AXL is in the cytoplasm can be used to identify subsets of conventional RCC with a high risk of progression.[21] Kyohei Hakozaki *et al.*[22] reported that different models of AXL and GAS6 expression were kept an eye out for original RCC and metastases, and the AXL/GAS6 scoring system could predict the prognostic outcome and serve as a powerful biomarker of RCC immunogenomic state. Andrew W Hahn *et al.*[21] revealed that a high AXL expression was associated with adverse reactions to anti-programmed death (PD)-1 therapy and increased tumor PD-L1 expression, and patients with a high AXL and PD-L1 expression have a particularly poor prognosis. For these reasons, as the potential biomarker and therapeutic target, AXL has become a research hotspot. In this study, AXL overexpression was detected in RCC cells, and the downregulation of AXL by siRNA was found to inhibit RCC cell proliferation, migration, and invasion. These research works were consistent with the consequence of the study by Yu.[11] They also further proved that AXL regulates certain physiological processes of RCC by activating PI3K/AKT signaling.

PI3K/AKT pathway is one of the most frequently activated intracellular pathways. PI3K/AKT is commonly considered as a balancer for human cancer.[23] This has been connected in promoting the regulation of various cellular physiological processes, particularly the proliferation, invasion, and apoptosis of carcinoma.[24] PI3K/AKT signaling is considered to be a key player in renal carcinogenesis, particularly in

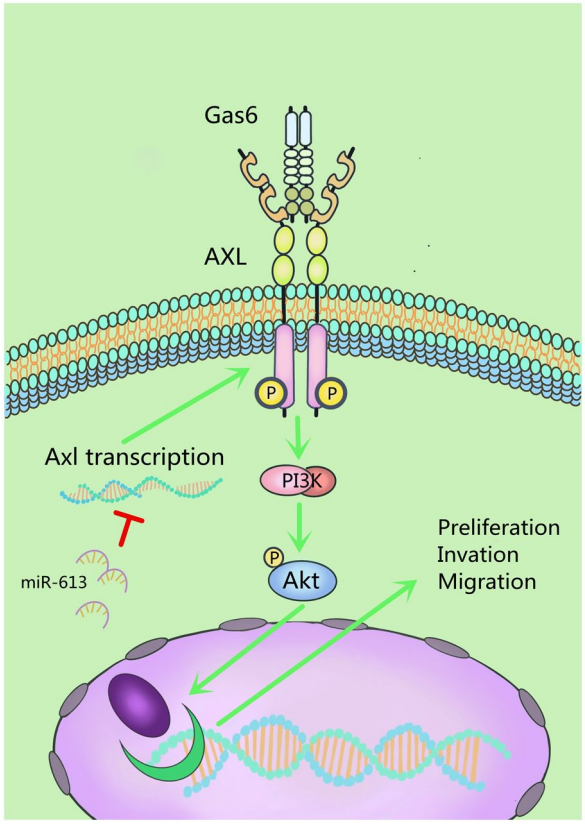

Figure 9. The miR-613/AXL/PI3K/AKT regulation axis in RCC progression is depicted schematically. AXL overexpression was found to activate the PI3K/AKT signaling pathway, promoting RCC progression. Furthermore, miR-613 can bind to the AXL 3'-UTR and inhibit AXL expression, preventing AXL-mediated PI3K/AKT signaling activation.

the histology of renal carcinoma. AKT, a serine/threonine kinase, is the pathway's most binding downstream component and is involved in signal transduction throughout the signaling cascade.[25] In RCC patients, the PI3K/AKT signaling remains the major focus in clinical research.[26]

MicroRNAs are a kind of non-coding RNA, which molecule has been measured 22 nucleotides in length.[27] miRNAs function as multiple tumor suppressors or carcinogens during tumor development. After extensive studies, miRNAs will be possible to effectively control and treat cancer.[28–33]

miR-613 is a newly discovered miRNA. There is increasing evidence that miR-613 is implicated in all sorts of physiological and pathological courses. Recent research works have illustrated that miR-613 is irregularly produced in different types of cancer. Meanwhile, miR-613 is great effective in the process of growth for carcinomas.[10,34–36] Concretely, miR-613 is considered to act as a cancer inhibitor in several types of tumors, including RCC.[37] Considering the heterogeneity of tumors and the ability of specific miRNA molecules to target different mRNAs, the same miRNA may exhibit differential effectors in the occurrence and development of different tumors. miR-613 acts as an oncogene in colon[38] and cervical[39] cancer and has been shown to promote cell proliferation, invasion and migration.

miR-613 has been shown to have an effect on RCC. Haitao Song *et al.*[8] demonstrated that by targeting and inhibiting FZD7, miR-613 acts as a tumor suppressor, inhibiting RCC cell proliferation and invasion.[8] Guanghui Hu *et al.*[40] revealed that miR-613 mimics should downregulate CXCR4 mRNA and suppress the Jagged1/Notch pathway in RCC. Nevertheless, given that each miRNA has multiple potential targets, one big issue in known functional miRNA impressions in cancerous cell behaviors ties to discern veritable molecular targets.[41] Therefore, the effect of the biological function of miR-613 on the cellular mechanism of RCC was elucidated herein. Last but not least, based on the bioinformatics results, it was found herein that AXL may be the target gene of miR-613, through inhibiting AXL, and miR-613 blocks PI3K/AKT signaling.

In a nutshell, these current findings indicated the expression of miR-613, in RCC, was dramatically reduced. In addition, in RCC cells, the current research confirmed the upregulation of miR-613 can control cell proliferation, metastasis, and invasion by reducing AXL levels and controlling the PI3K/AKT signaling pathway (Figure 9). Therefore, outcomes in this current research indicated miR-613 might be a potential therapeutic target for RCC, which may be available in the therapy of advanced RCC in future.

AUTHORS' CONTRIBUTIONS

WD analyzed data and edited the manuscript. SP collected data, analyzed data, and wrote the manuscript. YZ edited the manuscript. QD collected and analyzed data. WR and CD analyzed data. YS designed the study, edited the manuscript, and coordinated the project.

DECLARATION OF CONFLICTING INTERESTS

The author(s) declared no potential conflicts of interest with respect to the research, authorship, and/or publication of this article.

ETHICAL APPROVAL

Experiments using human tissue samples were approved by the Ethics Committee of Shaanxi Provincial People's Hospital (Xi'an, China; grant no. 2018K016). All participants signed written informed consent.

FUNDING

The author(s) disclosed receipt of the following financial support for the research, authorship, and/or publication of this article: This work was supported by the Natural Science Foundation of Shaanxi Province (2020JQ-945), the Hospital Incubation Fund of Shaanxi Provincial People's Hospital (2020YXM-07), the Shaanxi Provincial People's Hospital Science and Technology Talent Support Program (2021LJ-10), and development program (2017ZDXM-SF-050).

ORCID ID

Yi Sun https://orcid.org/0000-0003-3719-1755

REFERENCES

1. Siegel RL, Miller KD, Fuchs HE, Jemal A. Cancer statistics, 2021. *CA Cancer J Clin* 2021;**71**:7–33
2. Siegel RL, Miller KD, Jemal A. Cancer statistics, 2020. *CA Cancer J Clin* 2020;**70**:7–30
3. Karakiewicz PI, Suardi N, Capitanio U, Isbarn H, Jeldres C, Perrotte P, Sun M, Ficarra V, Zigeuner R, Tostain J, Mejean A, Cindolo L,

Pantuck AJ, Belldegrun AS, Zini L, de la Taille A, Chautard D, Descotes JL, Shariat SF, Valeri A, Mulders PF, Lang H, Lechevallier E, Patard JJ. Conditional survival predictions after nephrectomy for renal cell carcinoma. *J Urol* 2009;**182**:2607–12
4. Fu X, Cui Y, Yang S, Xu Y, Zhang Z. MicroRNA-613 inhibited ovarian cancer cell proliferation and invasion by regulating KRAS. *Tumour Biol* 2016;**37**:6477–83
5. Li D, Li DQ, Liu D, Tang XJ. MiR-613 induces cell cycle arrest by targeting CDK4 in non-small cell lung cancer. *Cell Oncol* 2016;**39**:139–47
6. Ren W, Li C, Duan W, Du S, Yang F, Zhou J, Xing J. MicroRNA-613 represses prostate cancer cell proliferation and invasion through targeting Frizzled7. *Biochem Biophys Res Commun* 2016;**469**:633–8
7. Ji Q, Xu X, Li L, Goodman SB, Bi W, Xu M, Xu Y, Fan Z, Maloney WJ, Ye Q, Wang Y. miR-216a inhibits osteosarcoma cell proliferation, invasion and metastasis by targeting CDK14. *Cell Death Dis* 2017;**8**:e3103
8. Sang Q, Liu X, Sun D. Role of miR-613 as a tumor suppressor in glioma cells by targeting SOX9. *Onco Targets Ther* 2018;**11**:2429–38
9. Ji H, Hu NJ. MiR-613 blocked the progression of cervical cancer by targeting LETM1. *Eur Rev Med Pharmacol Sci* 2020;**24**:6576–82
10. Huang Y, Zhang H, Wang L, Liu C, Guo M, Tan H, Liu Z. MiR-613 inhibits the proliferation, migration, and invasion of papillary thyroid carcinoma cells by directly targeting TAGLN2. *Cancer Cell Int* 2021; **21**:494
11. Yu H, Liu R, Ma B, Li X, Yen H-Y, Zhou Y, Krasnoperov V, Xia Z, Zhang X, Bove AM, Buscarini M, Parekh D, Gill IS, Liao Q, Tretiakova M, Quinn D, Zhao J, Gill PS. Axl receptor tyrosine kinase is a potential therapeutic target in renal cell carcinoma. *Br J Cancer* 2015;**113**: 616–25
12. Barata PC, Rini BI. Treatment of renal cell carcinoma: current status and future directions. *CA Cancer J Clin* 2017;**67**:507–24
13. Miricescu D, Balan DG, Tulin A, Stiru O, Vacaroiu IA, Mihai DA, Popa CC, Papacocea RI, Enyedi M, Sorin NA, Vatachki G, Georgescu DE, Nica AE, Stefani C. PI3K/AKT/mTOR signalling pathway involvement in renal cell carcinoma pathogenesis (Review). *Exp Ther Med* 2021;**21**:540
14. Rajeshkumar NV, Tan AC, De Oliveira E, Womack C, Wombwell H, Morgan S, Warren MV, Walker J, Green TP, Jimeno A, Messersmith WA, Hidalgo M. Antitumor effects and biomarkers of activity of AZD0530, a Src inhibitor, in pancreatic cancer. *Clin Cancer Res* 2009;**15**:4138–46
15. Gay CM, Balaji K, Byers LA. Giving AXL the axe: targeting AXL in human malignancy. *Br J Cancer* 2017;**116**:415–23
16. Zajac O, Leclere R, Nicolas A, Meseure D, Marchiò C, Vincent-Salomon A, Roman-Roman S, Schoumacher M, Dubois T. AXL controls directed migration of mesenchymal triple-negative breast cancer cells. *Cells* 2020;**9**:247
17. Okura N, Nishioka N, Yamada T, Taniguchi H, Tanimura K, Katayama Y, Yoshimura A, Watanabe S, Kikuchi T, Shiotsu S, Kitazaki T, Nishiyama A, Iwasaku M, Kaneko Y, Uchino J, Uehara H, Horinaka M, Sakai T, Tanaka K, Kozaki R, Yano S, Takayama K. ONO-7475, a novel AXL inhibitor, suppresses the adaptive resistance to initial EGFR-TKI treatment in EGFR-mutated non-small cell lung cancer. *Clin Cancer Res* 2020;**26**:2244–56
18. Nakada M, Kita D, Teng L, Pyko IV, Watanabe T, Hayashi Y, Hamada J-I. Receptor tyrosine kinases: principles and functions in glioma invasion. *Adv Exp Med Biol* 2020;**1202**:151–78
19. Yu W, Ge X, Lai X, Lv J, Wang Y. The up-regulation of Axl is associated with a poor prognosis and promotes proliferation in pancreatic ductal adenocarcinoma. *Int J Clin Exp Pathol* 2019;**12**:1626–33
20. Jeong I, Song J, Bae SY, Lee SK. Overcoming the intrinsic gefitinib-resistance via downregulation of AXL in non-small cell lung cancer. *J Cancer Prev* 2019;**24**:217–23
21. Hahn AW, George DJ, Agarwal N. An evolving role for AXL in metastatic renal cell carcinoma. *Clin Cancer Res* 2021;**27**:6619–21
22. Hakozaki K, Tanaka N, Takamatsu K, Takahashi R, Yasumizu Y, Mikami S, Shinojima T, Kakimi K, Kamatani T, Miya F, Tsunoda T, Aimono E, Nishihara H, Mizuno R, Oya M. Landscape of prognostic signatures and immunogenomics of the AXL/GAS6 axis in renal cell carcinoma. *Br J Cancer* 2021;**125**:1533–43
23. Shi X, Wang J, Lei Y, Cong C, Tan D, Zhou X. Research progress on the PI3K/AKT signaling pathway in gynecological cancer (Review). *Mol Med Rep* 2019;**19**:4529–35
24. Barra F, Evangelisti G, Ferro Desideri L, Di Domenico S, Ferraioli D, Vellone VG, De Cian F, Ferrero S. Investigational PI3K/AKT/mTOR inhibitors in development for endometrial cancer. *Expert Opin Investig Drugs* 2019;**28**:131–42
25. Rascio F, Spadaccino F, Rocchetti MT, Castellano G, Stallone G, Stefano Netti G, Ranieri E. The pathogenic role of PI3K/AKT pathway in cancer onset and drug resistance: an updated review. *Cancers* 2021;**13**:3949
26. Aurilio G, Santoni M, Massari F, Cimadamore A, Rizzo A, Mollica V, Verri E, Battelli N, Montironi R. Metabolomic profiling in renal cell carcinoma patients: news and views. *Cancers* 2021;**13**:5229
27. Winter J, Jung S, Keller S, Gregory RI, Diederichs S. Many roads to maturity: microRNA biogenesis pathways and their regulation. *Nat Cell Biol* 2009;**11**:228–34
28. Khan P, Ebenezer NS, Siddiqui JA, Maurya SK, Lakshmanan I, Salgia R, Batra SK, Nasser MW. MicroRNA-1: diverse role of a small player in multiple cancers. *Semin Cell Dev Biol* 2022;**124**:114–26
29. Elbadawy M, Usui T, Yamawaki H, Sasaki K. Emerging roles of C-Myc in cancer stem cell-related signaling and resistance to cancer chemotherapy: a potential therapeutic target against colorectal cancer. *Int J Mol Sci* 2019;**20**:2340
30. Chirshev E, Oberg KC, Ioffe YJ, Unternaehrer JJ. Let-7 as biomarker, prognostic indicator, and therapy for precision medicine in cancer. *Clin Transl Med* 2019;**8**:24
31. Gruszka R, Zakrzewska M. The oncogenic relevance of miR-17-92 cluster and its paralogous miR-106b-25 and miR-106a-363 clusters in brain tumors. *Int J Mol Sci* 2018;**19**:879
32. Beg MS, Brenner AJ, Sachdev J, Borad M, Kang YK, Stoudemire J, Smith S, Bader AG, Kim S, Hong DS. Phase I study of MRX34, a liposomal miR-34a mimic, administered twice weekly in patients with advanced solid tumors. *Invest New Drugs* 2017;**35**:180–8
33. Bader AG, Brown D, Stoudemire J, Lammers P. Developing therapeutic microRNAs for cancer. *Gene Ther* 2011;**18**:1121–6
34. Luo J, Jin Y, Li M, Dong L. Tumor suppressor miR613 induces cisplatin sensitivity in nonsmall cell lung cancer cells by targeting GJA1. *Mol Med Rep* 2021;**23**:385
35. Su X, Gao C, Feng X, Jiang M. miR-613 suppresses migration and invasion in esophageal squamous cell carcinoma via the targeting of G6PD. *Exp Ther Med* 2020;**19**:3081–9
36. Liu C, Jiang Y, Han B. miR-613 suppresses chemoresistance and stemness in triple-negative breast cancer by targeting FAM83A. *Cancer Manag Res* 2020;**12**:12623–33
37. Mei J, Xu R, Hao L, Zhang Y. MicroRNA-613: a novel tumor suppressor in human cancers. *Biomed Pharmacother* 2020;**123**:109799
38. Yang X, Zhang L, Song X, He W, Zhang D, Lu Q, Wu J, Wu C, Jiang J. MicroRNA-613 promotes colon cancer cell proliferation, invasion and migration by targeting ATOH1. *Biochem Biophys Res Commun* 2018;**504**: 827–33
39. Li WT, Wang BL, Yang CS, Lang BC, Lin YZ. MiR-613 promotes cell proliferation and invasion in cervical cancer via targeting PTPN9. *Eur Rev Med Pharmacol Sci* 2018;**22**:4107–14
40. Hu G, Ma J, Zhang J, Chen Y, Liu H, Huang Y, Zheng J, Xu Y, Xue W, Zhai W. Hypoxia-induced lncHILAR promotes renal cancer metastasis via ceRNA for the miR-613/206/ 1-1-3p/Jagged-1/Notch/CXCR4 signaling pathway. *Mol Ther* 2021;**29**:2979–94
41. Han N, Li H, Wang H. MicroRNA-203 inhibits epithelial-mesenchymal transition, migration, and invasion of renal cell carcinoma cells via the inactivation of the PI3K/AKT signaling pathway by inhibiting CAV1. *Cell Adh Migr* 2020;**14**:227–41

(Received August 25, 2022, Accepted December 11, 2022)